

A System for Live Localization In Smart Environments

Benjamin Wagner, Björn Striebing and Dirk Timmermann
Institute of Applied Microelectronics and Computer Engineering
University of Rostock
Rostock, Germany
firstname.lastname@uni-rostock.de

Abstract—The localization and tracking of users is an important part of sensing in smart environments. Superimposed intention recognition systems often rely on accurate user positions.

In device-free localization systems (DFL) users do not need to wear any hardware in order to be located. In RF systems they can be localized using the changes in signal strength measured on static communication links. Recent work has shown that a combination of completely passive RFID hardware and a tomographic imaging approach can achieve a mean location error as low as 0.3 m in a post-processed validation.

This work presents a system which is able to track the user in a live (online) mode with a constant frame rate while maintaining high accuracy. Conducting data from a demonstration setup the proposed system is able to locate users with a frame rate as low as 500 ms and a mean location error of 0.3 m.

Keywords—RFID, User Localization, Received Signal Strength, RSSI, Smart Environments, Positioning, Wireless

I. INTRODUCTION

The aim of today's research in the field of user localization for smart environments is creating inexpensive, wireless, privacy preserving systems. Compared to sensor localization methods only a few research has been done in the field of device-free user localization (DFL). Using these systems no hardware needs to be attached to the user. This area typically utilizes an environment equipped with active radio devices.

One approach is the *Radio Tomographic Imaging* technique (RTI) developed by Wilson and Patwari[1], [2]. The authors apply an imaging approach onto active sensor nodes which are placed around a measurement area. A person moving within this area is attenuating the signal strength values of the radio communication links. This gives information about the location and the movement of the user.

Based on that technique an innovative alternate approach is investigated at the University of Rostock within the Graduate School MuSAMA. Enhancing the inexpensiveness for device-free localization of users the active sensor node infrastructure is replaced by completely *passive Radio Frequency Identification* transponders (RFID) and only a few active RFID reader antennas. This leads to key advantages regarding the costs, because the price for passive RFID hardware is very low: transponders can be purchased for ~ 0.20 € and only few RFID readers are required. Additionally passive transponders do not need power from batteries, and can be easily placed in

the whole room, i.e. under the carpet or wallpaper.

However the new localization approach is achieving its performance only in an extensive data post-processing, although most applications of DFL require live (online) operation. The new system presented in this work extends the low cost and low maintenance approach with live operation maintaining high accuracy.

This paper is structured as follows: in Section II the related approach is described. Section III gives information about the system and time analysis. In Section IV methods and parameters are optimized for online operation followed by the description of the implementation in Section V. We conclude with Section VI.

II. RELATED WORK

Dealing with the reduction of high energy consumption and high deployment costs a new device-free user localization approach is subject to research in the graduate school MuSAMA[3]. The innovative idea is the replacement of typically used active antennas for RF-localization by completely passive *Radio Frequency Identification* transponders (RFID). Recent work has shown that high accuracies are possible using that technology[3].

The method *Radio Tomographic Imaging* (RTI) by Wilson and Patwari[1], [2] utilizes active wireless sensor nodes for device free user localization. An experimental area is defined by an image vector consisting of n pixels. When a person is affecting specific links in that network, the attenuation is regarded as the sum of attenuation each pixel contributes.

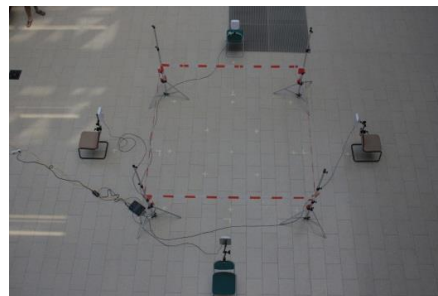


Fig. 1: RFID Deployment

Recently these two approaches were combined into a new approach called *Passive RFID Tomographic Imaging* [3]. Waist-high mounted passive transponders are placed around the localization area (cp. Fig. 1). The transponders are attached to white-red colored tape around the measurement

area. The four RFID antennas are placed behind the tag lines and measure the signal strength of the deployed transponders. For evaluation the difference of calibration and measurement value is used:

$$\Delta P = P_{meas} - P_{cal} \quad (1)$$

with P denoting the scaled signal strength value and ΔP the vector of RSSI differences. The calibration value as averaged in an offline calibration phase. The resulting image is calculated by using the model of Wilson et.al.[2]:

$$\Delta y = W \Delta x + n \quad (2)$$

with Δy as matrix of RSS differences in dB, W as pre-calculated weighting matrix for every pixel-link-combination, n as zero mean gaussian noise vector and Δx as matrix of pixel attenuations in dB creating the tomographic image. Fig. 2 shows sample images of the algorithm.

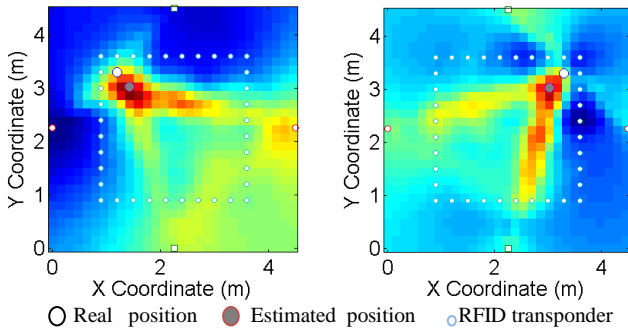


Fig. 2: Passive RFID Tomographic Images

For getting a user position in this method simply the center of the pixel with the maximum value is used. This is done due to the assumption that highest attenuation is bundled in the area of that pixel. Fig. 3 is showing the CDFs of the localization area out of 3 different user positions. Integrating a-priori knowledge about the users location (i.e. the user can only move within the transponder square) the precision could be increased. Overall the algorithm can locate human with as low as 0.3 m mean location error.

III. SYSTEM ANALYSIS

A. Architecture

The proposed localization system illustrated in Fig. 4 contains three major parts: the passive UHF RFID system, a network layer and the processing station. For our purpose a bistatic UHF reader working in the ISM 868 MHz band is used. The interrogator-transponder communication is realized with four linear polarized UHF antennas with a gain of 6 dBiL and a 70 degree azimuth beamwidth. We use a square field of side-mounted UHF transponders with a 96-bit EPC[4] compliant memory holding a unique identification number.

The RFID system communicates with an operating workstation over ethernet. Every tag-interrogator communication is repeated via network packets to the workstation for further evaluation.

The workstation is a Unix-PC with an Intel®Core™2 Quad CPU @ 4*3GHz.

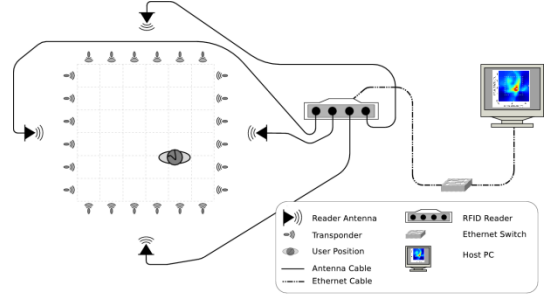


Fig. 4: System Architecture

B. Time Analysis

The main application scenarios of commercial RFID systems are logistics. In that area time is not the critical parameter. It is simply the distinction between a visible or invisible tagged object. Therefore every EPCglobal[4] compliant RFID system works according to hard implemented protocols in order to provide a maximum detection rate. Hence it is not able to work under defined real-time conditions. Furthermore the other system parts need to be looked at from the time point of view. Therefore we did a time analysis to get an idea about the reachable online capability and critical devices in the system. To implement a fix frame rate for the imaging algorithm we need to define a soft deadline for field measurements. The choice of the right deadline is a trade-off between a high frame rate and a high amount of measured data.

Within a fix deadline $t_{deadline}$ the system has to measure a sufficient number of antenna-transponder combinations, transmit the data to the workstation and process the imaging algorithm:

$$t_{deadline} \geq t_{acquire} + t_{network} + t_{calculate} \quad (3)$$

The time to fetch the measurement vector can be calculated as the product of interrogating antennas and the sum of powering and sequence changing time:

$$t_{acquire} = n_{tx} * (t_{transmit} + t_{as\ change}) \quad (4)$$

where the powering time is the product of the mean time between transponders reading for every transponder-antenna combination:

$$t_{transmit} = n_{rx} * n_{transponder} * t_{mean\ read} \quad (5)$$

The transportation time between measurement setup and localization algorithm consists of latency due to the ethernet protocol and the time for the tag streaming process and the import into the analysis software:

$$t_{network} = t_{latency} + t_{import} \quad (6)$$

According to (3) the single components have a different impact on the frame rate. Due to a multithreaded implementation of the software system image calculation and measurement process are working parallel. Hence the network time only leads to a constant imaging bias and has no effect on

the frame rate, which can be considered as the maximum between measuring time and image calculation time. As described in III.A we define a rolling measurement window with the length of one field edge. Hence we can reduce measurement time by coupling new measurement values with older ones. Hence the frame rate can be considered according to:

$$t_{frame} = \max \left\{ \frac{1}{n_{tx}} t_{acquire}, t_{calculate} \right\} \quad (7)$$

For demonstration purposes we aimed at implementing the highest possible frame rate into our system. A practical analysis of the time components is listed in Tab. 1 targeted at constraints of $t_{acquire}$ at first. According to (3) acquiring a complete RSSI vector needs transponders from all edges to be read. Since we can produce a frame after reading a single edge all measurements were applied on one edge reading all 10 transponders at the same time. From 100 measured cycles shown in Fig. 5 we can estimate a mean cycle duration of $t_{transmit}$ of ~240ms.

Parameter	Specification	Mean
$t_{acquire}$	fetch time for complete RSSI vector	1760 ms
$t_{network}$	time between reading and processing	110 ms
$t_{calculate}$	calculation time for imaging vector	77 ms
$t_{transmit}$	interrogator-transponder powering time	240 ms
$t_{as\ change}$	antenna sequence shifting time	200 ms
$t_{mean\ read}$	mean time between two transponder readings	25 ms
$t_{latency}$	ethernet network latency	0 ms
t_{import}	tag streaming latency and import buffer time	110 ms
t_{frame}	time per visualization frame	500 ms
n_{tx}	number of transmitting antennas	4
n_{rx}	number receiving antennas	1
$n_{transponder}$	number of available transponders	10

Tab.1: Time components

Changing the readers transmitting and receiving antenna requires approximately another 200ms as shown in Fig. 5.

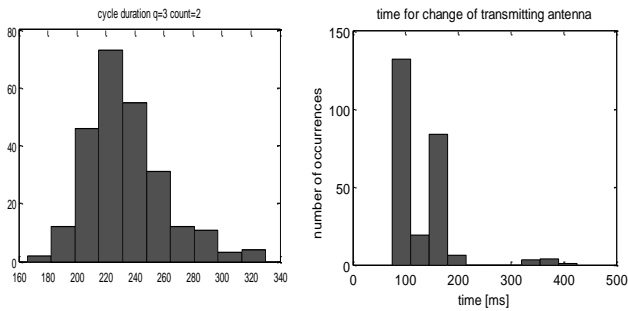


Fig.5: Mean cycle duration and antenna change time

Noticeable longer durations between two cycles are caused by a non-optional listen before talk (LBT) protocol integrated into the reader firmware. These results lead to a $t_{acquire} = \sim 440$ ms. Calculating the resulting image took about 77ms on our workstation. To avoid frequent deadline misses we decided to set the target frame rate to 2 fps or a new image every 500ms. With a negligible network latency of $t_{latency} <$

1ms we found a mean import time $t_{import} = 110$ ms which represents an additional bias as pointed out above. Tab. 1 summarizes the key time components determined with our analysis.

IV. SYSTEM OPTIMIZATION

A. Antenna Sequence

The key advantage of a bistatic passive RFID system is the ability to choose interrogating and listening antennas separately. On the one hand the antennas have a 2 dB lower attenuation while acting only as transmitter or receiver. Secondly you can separate between forward and backward communication link. The choice of the number and the type of sequence is an essential parameter for the overall localization performance. A higher number of tag-antenna combination leads to a higher amount of information, while the measurement time increases just as well.

Due to Lieckfeldt et.al.[5] the downstream contains more than twice the information than the uplink. Therefore we considered the uplink simply as power source for the transponder without any information. We defined an antenna sequence as:

$$AS = \{0,1; 2,3; 1,0; 3,2\} \quad (8)$$

where the first parameter denotes the interrogating and the second the listening antenna.

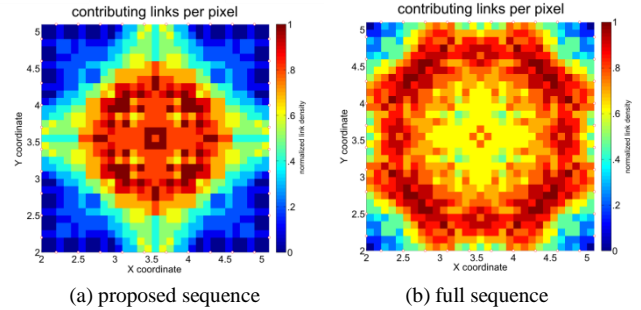


Fig. 6: Link density comparison

The imaging algorithm is based on pixel value calculation, where pixels are contributed to influenced links over a weighting matrix. Assuming the link density per pixel Fig. 6 is showing the density images for all possible antenna sequences vs. our proposed sequence. The original approach assumes a uniformly distributed link density on the capturing field. In [3] we show that the influence on the localization precision is not as high. Comparing the two density scenarios it is obvious that a smaller sequence leads to a higher fluctuation in the link density image.

B. FSA and EPC Parameters

Key parameters of an EPCcompliant UHF RFID system are the adjustment parameters of the implemented anti-collision communication protocol utilizing a *frame slotted ALOHA* (FSA). Therefore three main parameters are to be faced (cp. Tab. 2). In the defined measurement scenario we work with $n_{transponder} = 40$ side mounted transponders. In one reading

cycle (one antenna combination) the antenna in the direct back of the transponders is powering ten transponders of one row in front of it.

Parameter	Specification
Cycles	number of inventory rounds for every tx rx pair
Count	number of frames per inventory
Q	time slots per frame

Tab.2: FSA parameters

Hence there are always ten transponders in direct competition for communication slots of the FSA protocol.

Finkenzeller[6] and Kawakita[7] define the optimal frame number according to the number of participants as:

$$Q = \log_2(n_p) \quad [6] \quad (9)$$

The authors also provide arguments that this could only serve as a reference, because the number of unlisted transponders is constantly increasing.

In our implementation the RFID software works with an automatically antenna sequence shifting, hence we can choose cycles = 1.

FSA		$t_{transm}[ms]$			n_{rcod}	
q	count	\bar{t}	t_{min}	t_{max}	$[cycle^{-1}]$	$[s^{-1}]$
1	1	238,4	154,0	363,0	9,21	25,26
3	1	237,8	178,0	412,0	9,23	26,03
3	2	234,4	166,0	330,0	9,24	24,57
4	1	239,5	167,0	354,0	9,18	25,74

Tab.3: FSA evaluation

As you can see in Tab. 3 we have a mean number of listed transponders of 9,2 transponders per inventory round which is enough for our 10 transponder row. The optimal mean transmitting time with ~238 ms is low enough for a frame rate of minimum 2 images per second (due to antenna shifting).

C. Algorithm Parameter

As mentioned in [3] there is a number of different adjustment parameters with a direct impact on the imaging result shown in Tab. 4.

Parameter	Specification
δ	width of covariance matrix
σ	weighting factor for covariance term
λ	elliptic width for weighting matrix

Tab.4: Tomography adjustment parameters

As we want to create an online capable system we have to deal with a decreasing dataset size and due to that with less information. In [3] we had the chance to take available data of every antenna-transponder combination and do the evaluation in a post-processing step. As we do not have that time we need to optimize the imaging parameters to get the best possible imaging performance out of the available data.

The covariance[3] values for different widths are shown in Fig.7. As you can see the pixel-pixel interdependence is

decreasing with a smaller width. In Fig.8 you can see the influence of δ on the systems accuracy. We choose a $\delta=10$ because of significant rise of accuracy.

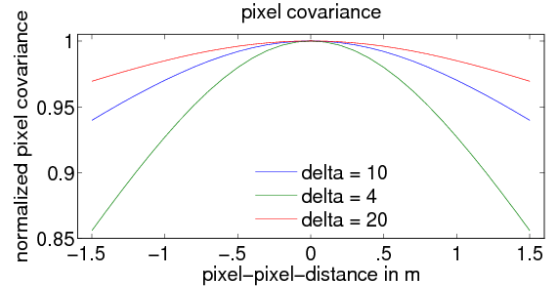


Fig.7: pixel covariance

Fig. 9 is showing the impact of weighting factor σ on the localization accuracy with a maximum near 0.001 which is the value we will use for further evaluation.

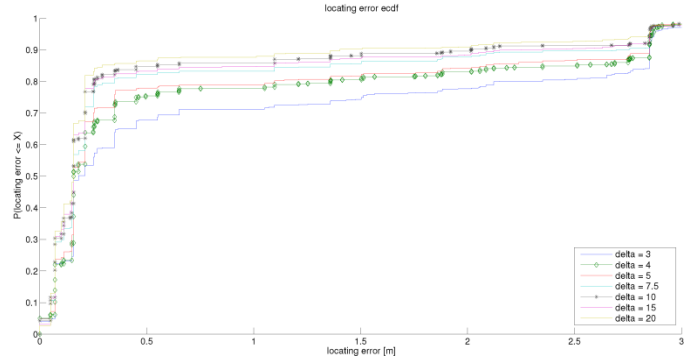


Fig.8: ECDF for covariance width values

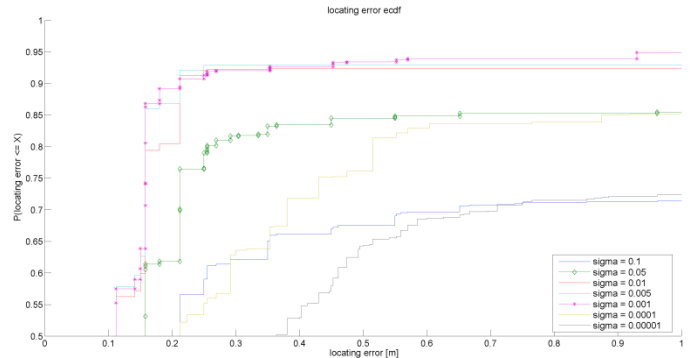


Fig.9: ECDF for weighting values

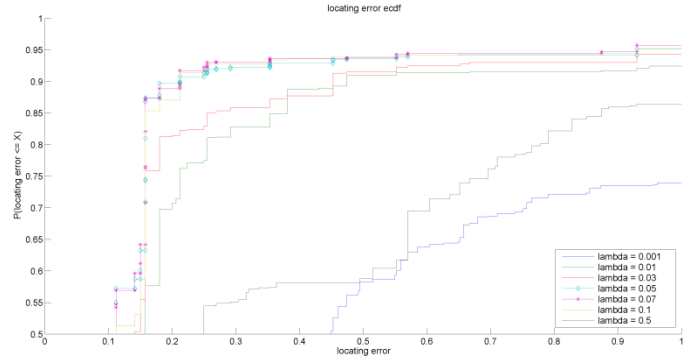


Fig.10: ECDF for elliptic width values

The last investigated parameter is the width of the elliptic LOS curve for the weighting matrix generation. A higher value will adjust more contributing pixel to one LOS communication path and result in a stronger impact of the attenuation on the resulting image. Since the derivation of user positions out of the calculated image is pixel based, a variation of the weighting matrix has direct effect on the localization performance. In Fig. 10 an optimal value of ~ 0.07 is legible, due to this particular experimental scenario. A changing layout needs a complete recalibration.

D. Weighting Matrix

The weighting model generates a weighting value for every link-pixel combination (cp. Fig.11). Pixels in the direct Line-of-sight (LOS) path have a higher influence on the RSS shadowing, than the pixels around[3]. Considering the separated communication paths of a typical RFID system and the proposed experimental scenario, the forward link can be regarded only as power source for the transponder set.

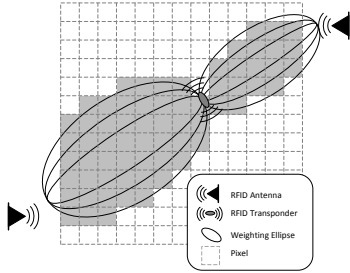


Fig.11: Adaptive Pixel Weighting Model

Hence only the backward link will be subject to further investigations. In equation (10) to (12) we provide three different weighing models based on an elliptic curve on the LOS path. In (10) a *constant weighting factor* is applied on all

$$W_{ij \text{ downlink}} = \begin{cases} 1 & \text{if } d_{z(i) j} + d_j \text{ rx}(i) < d_{z(i) \text{ rx}(i)} + \lambda_{\text{downlink}} \\ 0 & \text{else} \end{cases} \quad (10)$$

$$W_{ij \text{ downlink}} = \begin{cases} \frac{n_{\text{link reads}}}{n_{\text{total reads}}} & \text{if } d_{z(i) j} + d_j \text{ rx}(i) < d_{z(i) \text{ rx}(i)} + \lambda_{\text{downlink}} \\ 0 & \text{else} \end{cases} \quad (11)$$

$$W_{ij \text{ downlink}} = \begin{cases} \frac{1}{\sigma_{\text{link}}} & \text{if } d_{z(i) j} + d_j \text{ rx}(i) < d_{z(i) \text{ rx}(i)} + \lambda_{\text{downlink}} \\ 0 & \text{else} \end{cases} \quad (12)$$

pixels lying within the elliptic curve adjustable by parameter λ . Typically the systems process is consisting of two major parts: a calibration phase and an operation phase. Transponders which have bad read results in calibration typically provide less reliable information. Therefore we proposed a *relative frequency weighting factor* in (11). Finally we provide a *variance based pixel weighting* due to the fact, that a lower link variance could be regarded as a better readable transponder. As you can see in Fig. 12 constant and relative weighting factors performs very well while variance based weighting factors decrease the localization accuracy.

This could be explained by regarding less information due to suppressed LOS links.

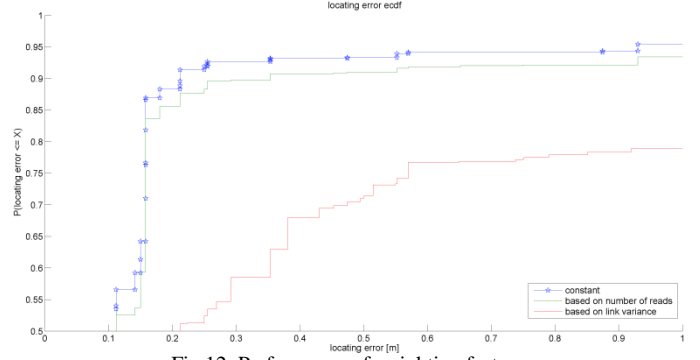


Fig.12: Performance of weighting factors

E. Threshold Based Position Estimation

One great opportunity of imaging algorithms is the manual comprehensibility of the calculated pictures. Typically the tomography pictures show a certain hotspot area which contains the most probable user location. In recent approaches simply the center of the maximum value pixel was regarded as result. Due to high measurement uncertainties in the commercial RFID hardware this result is not reliable enough. Therefore we implemented a *threshold based centroid estimation* method. A threshold provides a certain pixel area which an attenuation high enough above the measurement error. We have two possibilities to set this threshold:

- *Dynamic threshold*: relative signal strength value due to maximum pixel attenuation
- *Link density*: individual pixel threshold due to its crossing LOS links

After applying this threshold on the measured data matrix we obtain a set of pixels with a high probability of user presence. About calculating the centroid of this pixel area a user location can be estimated. These mathematical operations can be done very fast. Fig.13 shows the localization results due to different threshold values. A maximum accuracy can be reached with 75 % of the maximum signal attenuation. A lower threshold leads to a higher center based bias, a higher value is preferring a single maximum pixel.

F. Backcoupling and Framerate

As described above in chapter III the frame rate t_{frame} is dependent on the measurement time. A higher measurement is reducing the frame rate and the information amount for position estimation. To meet this problem we propose a combination of new measuring data and older weighted data. In the described setup all 4 field lines have to be measured ($4 \times t_{\text{frame}}$). We defined a minimum of 500 ms for t_{frame} as a compromise between a possible user movement and online capability. To do this we generate a dynamic weighting matrix for the whole measurement vector and apply it by a back coupling factor α . New measurement values are weighted by $\alpha - 1$ to implement a low-pass behavior to meet high measurement fluctuations.

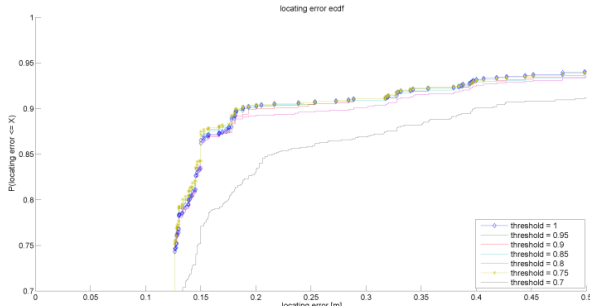


Fig. 13: localization estimation

The decreasing impact of older values is illustrated in Fig. 14. Implementing this we can calculate our results continuously with a combination of old weighted and new measurement values and are independent of RFID communication delays.

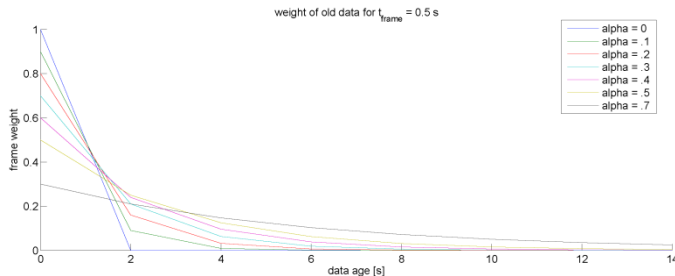


Fig. 14: Frame weight vs. Data age

Our results show that this method can be used very effectively to generate high accurate positioning results with acceptable frame rates. It has to be noticed that the low pass filter leads to a lower image dynamic. The results are shown in Fig. 15. For implementing an online demonstrator we found $\alpha = 0.4$ as an appropriate choice.

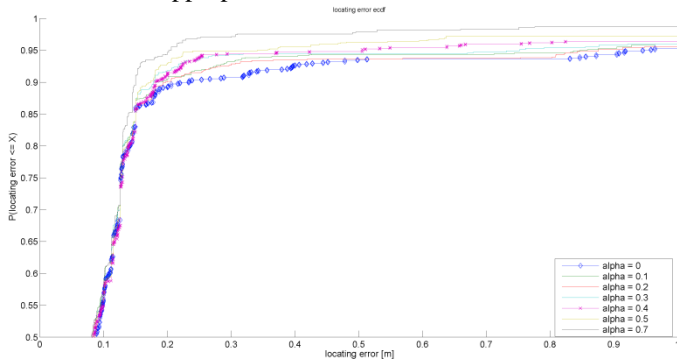


Fig. 15: Results of back coupling approach

V. DEMONSTRATOR

Using the described approaches we implemented an online capable user positioning demonstrator based on the proposed experimental setup and hardware. We implemented the algorithms in an integrated parallel software stack based on an Java Virtual Machine (JVM) and MATLAB®. An integrated Java thread realizes the RFID hardware communication and control and provides a graphical user interface (GUI) for system setting purposes. Fig. 16 shows a general system structure. In parallel with the java communication a Matlab script imports the data and runs the customized tomography algorithm.

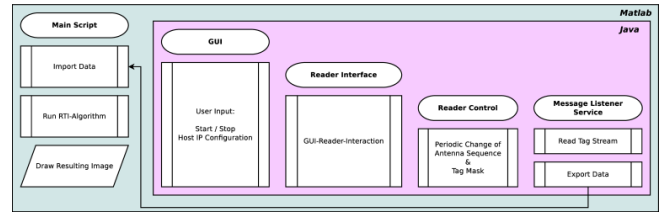


Fig. 16: Demonstrator structure

We deployed the setup in the atrium of the informatics building to reduce the impact of NLOS reflection from adjacent walls. The setup is shown in Fig. 1. A sample of the demonstrators output is outlined in Fig 17. A person moving around in the measurement area can be localized in a live mode (online) with mean localization error of $\sim 0.3m$.

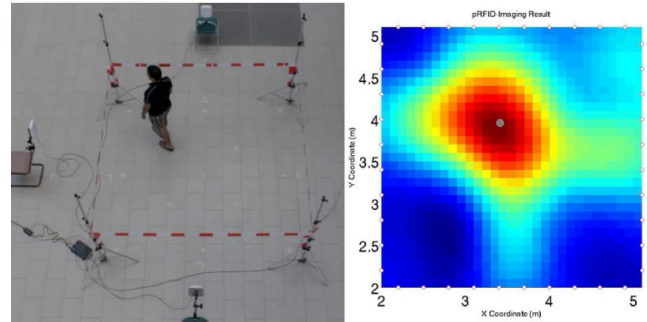


Fig. 17: Online Demonstration

VI. CONCLUSION

In this work we propose an online capable device free user localization system based on passive RFID and radio tomography. Utilizing the approach of Wagner and Patwari[3] a system was designed, which is able to do live localization utilizing a commercial off-the-shelf RFID system. Therefor an analysis for critical time components was done. After identifying critical time parts, system parameters were optimized regarding both frame rate and accuracy aims. The resulting system is easy to deploy with a multi-threaded software stack. An accuracy lower than 0.3 m can be achieved with a frame latency lower than 500 ms.

REFERENCES

- [1] J. Wilson and N. Patwari, "Through-Wall Motion Tracking Using Variance-Based Radio Tomography Networks," *arXiv.org*, Oct 2009.
- [2] J. Wilson and N. Patwari, "Radio Tomographic Imaging with Wireless Networks," *IEEE Transactions on Mobile Computing*, vol. 9, no. 5, pp. 621–632, May 2010.
- [3] B. Wagner and N. Patwari, "Passive RFID Tomographic Imaging for Device-Free User Localization," *Workshop of Positioning, Navigation and Communication*, no. 1, pp. 1–6, Dresden 2012.
- [4] EPCGlobal Inc., "Specification for RFID Air Interface EPC™ Radio-Frequency Identity Protocols Class-1 Generation-2 UHF RFID Protocol for Communications at 860 MHz – 960 MHz" October, 2008.
- [5] D. Lieckfeldt, J. You, and D. Timmermann, "Exploiting RF-Scatter: Human Localization with Bistatic Passive UHF RFID-Systems," *2009 IEEE International Conference on Wireless and Mobile Computing, Networking and Communications*, pp. 179–184, Oct 2009.
- [6] K. Finkenzeller, *RFID Handbook*. Carl Hanser Verlag, 2006.
- [7] Y. Kawakita, "Anti-collision performance of Gen2 Air Protocol in Random Error Communication Link," *International Symposium on Applications and the Internet Workshops (SAINTW'06)*, pp. 68–71, 2005.